NASA
Technical
Paper
2381

February 1985

Fluctuating Pressures on Fan Blades of a Turbofan Engine

Flight Test Investigation

James A. Schoenster

NASA

NASA
Technical
Paper
2381

1985

Fluctuating Pressures on Fan Blades of a Turbofan Engine

Flight Test Investigation

James A. Schoenster

Langley Research Center
Hampton, Virginia

NASA
National Aeronautics
and Space Administration

Scientific and Technical
Information Branch

Summary

Miniature pressure transducers were used to measure the fluctuating pressure on the fan blades of a JT15D engine in flight to aid in understanding fan-noise generation. Tests were conducted with the engine mounted on the wing of an OV-1B airplane that was flown at a speed of about 130 knots and at an altitude of about 91 m. Techniques used for interpreting the results include narrow-band spectral analysis and signal-enhancement analysis by using a precise measurement of the blade circumferential position as a reference. It was found in flight that the pressures at the harmonics of the blade passage frequency increase uniformly with increasing fan speed until transonic blade tip speeds are reached, at which time the amplitude of these signals then varies greatly. The one-per-revolution oscillation on the blades is very similar to the six-per-revolution oscillation on the blades, a result previously identified as a potential field effect from having six support struts in the duct, and is considered to be associated with a flow-field effect caused by the duct. Although the blade pressures can be considered very useful in determining far-field noise sources in the subsonic fan-blade tip speeds, other mechanisms, such as shock waves in the transonic and supersonic fan-blade tip speeds, limit their usefulness in these higher speed ranges.

Introduction

For several years, studies have been conducted to aid in understanding the mechanism of noise generated by the fan of a turbofan engine. Results from these studies demonstrated that measurements obtained from ground static tests differed from the noise measured in flight tests (e.g., ref. 1). One of the potential causes for this lack of agreement is the dissimilarity in turbulent inflow between ground tests and flight tests (ref. 2).

The purpose of this report is to present the results from fan-blade-mounted transducers obtained during flight and compare these results with those obtained during a wind-tunnel test. These measurements on the fan blade provided information at the potential source of the noise, and the comparisons are explored to help explain differences in far-field data.

Hanson (refs. 3 and 4) developed a unique data acquisition/reduction method designed to identify such variations by observing the pressures on the surface of the fan blades. In his work, miniature pressure tranducers were mounted on the surface of the fan blades and data from these transducers were analyzed as a function of angular location around the fan rotation plane. Although a direct application of these measurements to predict the far-field radiated noise has not yet been established, several characteristics of the noise mechanisms may be identified. Studies by Rogers and Ganz (ref. 5) evaluating the effectiveness of an inflow control structure used Hanson's method to compare data from static ground tests with flight data on a JT9D[1] engine. Fan-noise studies on a JT15D[2] engine (refs. 6 and 7) used this method to compare data from static ground tests with data from wind-tunnel tests in order to evaluate differences in far-field noise measurements.

Preliminary data from flight measurements of the fan-blade-mounted transducers were presented in references 8 and 9. In the present paper, a more comprehensive treatment is given to the data and the results are compared with results from a wind-tunnel test using the same engine. An evaluation of these measurements related to potential propagating modes out of the inlet duct is presented for fan tip speeds ranging from subsonic to supersonic. Data from these transducers are evaluated by using fan speed, spectral density, and angular position around the fan face.

Symbols

Values are usually given in SI Units and, where considered useful, also in U.S. Customary Units.

B	number of fan blades
f_n	fan rotational frequency, Hz
h	harmonic order of fan rotational frequency
m	mode number
N	total number of fan revolutions
P	pressure, Pa
P^*	pressure with instrumentation bias removed, Pa
Θ	total number of discrete, angular, fan-blade positions
σ	standard deviations of pressure, Pa

Subscripts:

n	number of fan revolutions
θ	angular position around inlet circumference, deg

Abbreviations:

ccw	counterclockwise
FFT	fast Fourier transform
freq	frequency

[1] Manufactured by Pratt & Whitney Commercial Products Division.

[2] Manufactured by Pratt & Whitney Aircraft of Canada.

ref reference

A bar over a symbol denotes the mean value.

Description of Experiment

Test Engine

The test engine, a modified JT15D turbofan, is a twin-spool, front-fan jet propulsion engine which has a full-length annular bypass duct. It has a nominal bypass ratio of 3.3 and a maximum thrust capability of 9790 N. (See table I for specifications.)

The fan is 53.3 cm in diameter and has 28 blades. (See figs. 1 and 2.) The fan is followed by a stator assembly, consisting of a bypass stator that has 66 vanes and a core stator that has 71 vanes. The latter is the only major difference between a production JT15D engine (which has 33 core-stator vanes) and the test engine. The modified core stator has more blades and is aft of the rotor blade root at a distance of 0.63 fan-blade root chord (compared with 0.28 root chord for a production engine) so that the fan-rotor/core-stator interaction tone was acoustically cut off and the broadband noise was diminished. The next rotating blade assembly is the compressor which is a combination axial-centrifugal compressor having 16 blades in the leading axial part of the unit.

As shown in figure 3, the engine core is supported by six internal struts that are located in the intermediate case of the engine. These supports traverse the compressor and bypass ducts to attach the core to the outer wall of the engine intermediate case. These struts are aft of the stator assembly, but in the bypass duct they are about 14 cm behind the trailing edge of the rotor blade tip. The struts at the top and bottom of the bypass duct are about 3.18 cm wide at their maximum thickness and 18 cm long, whereas the other four struts are 2.54 cm wide and 18 cm long. Both sets of struts taper in width to a relatively narrow trailing edge.

The engine operates over a range of fan speeds from about 6700 to 16 000 rpm. The ratio of inlet Mach number to fan-blade-tip Mach number increases from 0.28 to 0.34 in this range.

The test engine was fitted with a muffler to reduce the aft-radiated noise from the bypass duct. This was considered necessary to minimize any possible contamination of the measurements of front-radiated fan noise of interest in the present investigation. The muffler was designed so that the bypass and core exit areas remained the same as in an untreated engine.

A more extensive description of the engine and inlet performance may be found in reference 10.

Test Conditions

Flight. The JT15D engine was mounted on a wing pylon of an OV-1B airplane (fig. 4) and was flown over an array of microphones at a speed of about 67 m/sec (130 knots) at an altitude of about 91 m. During the data runs the airplane starboard engine (nearest the JT15D) was shut off and the propeller remained stationary. Altitude and speed were maintained by the port engine while the JT15D was held at a constant fan speed. The OV-1B is a U.S. Army observation airplane manufactured by the Grumman Aerospace Corporation. Details of the OV-1B/JT15D integration studies and of the resulting airplane performance and operational envelope are found in reference 11.

Wind tunnel. The same engine was mounted on a single strut that was 4.57 m above the floor of the Ames 40- by 80-Foot Wind Tunnel (fig. 5). The test-section floor and walls, in the immediate area surrounding the engine, were lined with a 7.62-cm-thick layer of acoustic foam. Tests were conducted for conditions ranging from the tunnel off to a simulated forward speed of 44 m/sec. Results presented in this paper are for the tunnel operating at 44 m/sec, and results in reference 7 are for the tunnel operating at several different speeds.

Instrumentation and Data Processing

Fan-blade-mounted transducers. Four miniature (1-mm-diameter sensing area) pressure transducers (denoted as G, H, I, and J) were bonded to the blade surface of one particular fan blade. Three transducers were located at the leading edge of the blade (5-percent-chord position): transducer G at 68 percent, transducer H at 88 percent, and transducer I at 96 percent of the blade span (fig. 6). One transducer (J) was located at 88-percent span length near the trailing edge at the 88-percent-chord position. The total thickness of the mounted transducer was less than 0.33 mm above the surface of the blade, including the rubberized bonding material which was used to fair the transducer to the curvature of the blade. Because of the uniqueness of this mounting arrangement, an evaluation of this system was conducted in reference 12. Effects such as temperature, static strain, oscillatory strain, centripetal acceleration, and oscillatory acceleration were evaluated (ref. 12), and it was concluded that the unsteady pressures on the fan blade could be satisfactorily obtained for this study. A photograph of the installation is presented in figure 7.

Signals from these transducers were transmitted from the fan hub to an antenna in the inlet duct wall and were recorded on an analog tape recorder. The system was designed to measure pressures in the range from 20 Hz to 20 kHz with a sensitivity of 0.145 mV/Pa (1 V/psi). The signal-to-noise ratio was 50 dB and the dynamic range was from 120 to 170 dB. These data were recorded as analog signals on alternate channels of a

magnetic tape recorder using a 108-kc carrier frequency and a tape speed of 30 in/sec. Details explaining the data acquisition system for these transducers may be found in reference 13.

Data processing. Fluctuating pressure data from the magnetic tapes were analyzed by using several procedures. An overview of the blade-pressure spectrum throughout the operating range of the engine was obtained to provide an insight to the general characteristics of the fan-blade pressure. This was accomplished by analyzing data from a test in which the fan speed was manually varied by slowly moving the throttle from its maximum operating position to its minimum position. By using a bandwidth of 10 Hz up to 5000 Hz, this signal was continuously analyzed in 256 averages per spectrum step, yielding a continuous stepped time history of the pressure spectra. The change in fan speed during any one step is about 5 Hz, or half the bandwidth of the analysis. Evaluation of these data provided aid in selecting fan speeds from those tested for additional analyses. Since the exact fan speeds were selected before the tests started, the choice of speeds for these additional analyses was limited.

The next data-analysis method follows a procedure developed by Hanson (e.g., ref. 4) to analyze data from transducers on rotating machinery. The method relates the measured pressure signal from the transducer with a precise measurement of the fan-blade position. This allows the data to be evaluated in terms of the angular position of the blade-mounted transducers. Thus, the measured pressure is analogous to the measurements of a continuous circular array of fixed transducers. For these tests, the blade-position sensor incorporates an optical sensor system which is triggered each time that a selected polished blade passes the sensor. This signal is converted into a 2-msec constant-amplitude pulse whose rising slope indicates the passing of the polished blade. This signal is recorded along with the pressure data, and the leading-edge trigger of this pulse provides an accurate indication (within 0.1°) that the instrumented blade is at the top dead-center position of the engine inlet.

With the pulsed signal as a reference (by using a tracking-ratio synthesizer), the pressure data are sampled at a rate of 360 points per revolution (independent of the fan speed). The amplitude range of the digitized signal is set at ±998 scale units per full-scale signal from the analog tape and is converted to engineering units by using the appropriate sensitivity for each transducer. As a preliminary analysis, these data are then divided into contiguous blocks of 1024 samples per block, which are processed through a fast Fourier transform (FFT) analysis program and averaged for 78 transforms. This analysis provides a spectrum of the pressure (before enhancement) in bandwidths of $0.35f_n$, where f_n is the fan rotational frequency.

The data are then ordered in the form $P_{n,\theta}$, where n is the number of fan revolutions (established from an arbitrary starting point) and θ is the number of the data point in a revolution (representing the angular position around the inlet circumference at which the measurement was obtained).

The mean value of the total data sample P is calculated by

$$\bar{P} = \frac{1}{N\Theta} \sum_{n,\theta=1}^{N,\Theta} P_{n,\theta} \tag{1}$$

where N and Θ were selected to be 1000 and 360, respectively. This value is subtracted from all the data points (i.e., $P^*_{n,\theta} = P_{n,\theta} - \bar{P}$) to remove any bias due to instrumentation.

The next step is to calculate the mean value of the deviation P_θ and the standard deviation σ_θ of the pressure signal as a function of angular position by using the following formulas with $N = 1000$:

$$\bar{P}_\theta = \frac{1}{N} \sum_{n=1}^{N} P^*_{n,\theta} \tag{2}$$

$$\sigma_\theta = \left[\frac{1}{N} \sum_{n=1}^{N} (P^*_{n,\theta} - \bar{P}_\theta)^2 \right]^{1/2} \tag{3}$$

These values are plotted as functions of blade angle.

The next step in this process is to take the first 250 revolutions and average the data as a function of angle θ; then, repeat this process with revolutions 251 to 500, revolutions 501 to 750, and revolutions 751 to 1000. This procedure results in four records with each being 360 data points long. By connecting these records one directly after the other, a single data trace of 1440 data points is formed and this trace is then spectrum analyzed. The result is a frequency analysis of the enhanced pressure in $0.25f_n$ increments of the harmonic orders of the fan rotational frequency.

Variations in the mean value of the deviation indicate a mechanism causing a deterministic spatial change in the static pressure around the circumference. The standard deviation is a measure of the magnitude of pressure fluctuations, either periodic or random, on the blade surface at a fixed angular position. A constant standard deviation around the entire circumference indicates uniform fluctuations per unit angle θ over the entire inlet, whereas variations in standard deviation around the circumference indicate that there is a mechanism causing a spatial distribution of the time-varying pressure levels over the inlet. In a comparison of the spectral analysis of the total signal with that of the enhanced signal, the signal is primarily periodic if at any frequency the enhanced signal is less than 3 dB below

the total signal at that frequency. A demonstration of this data-evaluation procedure may be found in reference 7.

Results and Discussion

The results of this study are presented in the following sequence. An overview of the frequency spectra in flight is presented for two transducers during a fan-speed variation from about 15 900 to 6400 rpm (fig. 8). The characteristics of the blade pressures are then presented for three fan-blade tip speed ranges during flight, corresponding to subsonic, transonic, and supersonic relative blade tip speeds. The relative fan tip speed was determined from the vector sum of the rotational speed of the fan blade and the duct inlet flow. The inlet speed at the fan face was determined by using the average static pressure measured in the inlet and the total static pressure of the airplane in flight following the procedure outlined in reference 10. The overall spectra, standard and mean deviations, and enhanced pressure spectra (harmonic orders) are used to show these characteristics for transducer H in figures 9, 10, and 11. In figure 12 the standard and mean deviations are presented for the trailing-edge transducer during subsonic, transonic, and supersonic blade-tip-speed conditions. The overall spectra, standard and mean deviations, and enhanced pressure spectra for this transducer are shown in figure 13 for the transonic range. Plots of the pressure amplitude (in dB) of the first, second, and sixth harmonic of the fan-blade passage frequency as a function of fan speed for all the transducers are shown in figures 14, 15, and 16. Results of transducers H and J in the transonic fan speed range are presented from the tunnel tests in figures 17 and 18, respectively.

Flight Tests

The effect of fan speed variation on the pressure spectra may be seen for transducers H and J (figs. 8(a) and 8(b), respectively). The initial peak in each of the spectra occurs at the fundamental rotational frequency of the fan. It may be seen that throughout the entire fan speed range, only a few peaks in the spectrum are observable. The first, second, and sixth harmonic of the fan speed are generally above the noise floor, that is, within 20 dB of the maximum peak value. Some other narrow-band peaks appear above the noise floor at various speeds but not over the entire speed range. Three regions of blade relative tip speed (subsonic (11 200 rpm and below), transonic (from 11 200 to 13 000 rpm), and supersonic (above 13 000 rpm)) are similar to those observed in reference 13. In the transonic blade tip speed range, as was noted in the tunnel, the broadband fluctuating pressure levels rose much higher at the leading edge (fig. 8(a)), almost obscuring the harmonics of the fan speed. At the trailing edge (fig. 8(b)), the broadband noise does not show in the spectra. At supersonic blade tip speeds, the broadband noise decreases and the harmonics then clearly dominate the spectrum both at the leading and trailing edges.

A closer look at the pressure responses in each of these regions may be seen in figures 9 to 11. Transducer H has been used to show the characteristics of the blade pressures. In figure 9(a) the overall spectra show the identifiable peaks equivalent to the 1st, 2d, 6th, and 66th harmonics of the fan rotational frequency. (The 66th harmonic did not show up in the fan sweep analysis because the range of analysis did not cover this frequency.) The 66th harmonic is related to the 66 stators in the bypass duct. Figure 9(b) presents the standard and mean deviations of the averaged pressure signals. The previously identified six cycles per revolution (ref. 12) associated with the six struts in the bypass duct are easily observable in the mean angular deviation plots. The standard deviation shows no sensitivity to angular position. Both the shape and levels of the mean and standard deviations agree very closely with those reported for the tunnel tests in reference 13. Similar to the tunnel tests, the harmonic-order analysis indicates that the observable peak responses in the spectral analysis (1st, 2d, 6th, and 66th) are primarily periodic in frequency and amplitude. (That is, the harmonic-order amplitude is within 1 dB of the spectral-analysis amplitude.)

Data in the transonic range (11 850 rpm) are shown in figure 10. At this fan tip speed the peaks in the overall spectra (fig. 10(a)) clearly show up at the fundamental fan frequency and the sixth harmonic; however, in the sweep test data at some transonic speeds, these amplitudes are somewhat masked by the large increase in the broadband fluctuating surface pressures (fig. 8(a)). The mean angular deviation (fig. 10(b)) shows a large increase in amplitude at the six-cycle frequency. A difference from the subsonic case is the increase in the standard deviation (fig. 10(b)), which now also varies in the six-cycle-per-revolution pattern seen in the mean angular deviation. The order analysis (fig. 10(c)) shows the amplitude of the first harmonic to be 150 dB and of the sixth harmonic to be 152 dB. The overall spectral analysis yielded an amplitude of 150 dB at the first harmonic frequency and of 153 dB at the sixth harmonic frequency. Although the standard deviation has increased, the signals at these frequencies are still predominantly periodic.

The pressure on the blade in the supersonic range (13 300 rpm) shows a high harmonic content in figure 11(a), a return to the lack of angular sensitivity of the standard deviation, and an observable six cycles per revolution in the mean angular deviation in figure 11(b). This six cycles per revolution occurs at a much lower

level than in the subsonic and transonic ranges. The amplitude at the harmonic orders of the fan speed are primarily periodic, as indicated by the harmonic-order analysis in figure 11(c).

The mean- and standard-deviation analyses for the trailing-edge transducer J are shown in figure 12. In the subsonic range (10 400 rpm), the pattern is similar to that for transducer H (fig. 9). However, in the transonic range (around 11 850 rpm), some differences are observable. For example, the standard deviation does not increase as significantly for transducer J as for transducer H (fig. 10), and a pronounced angular variation around the circumference does not occur. In addition, an oscillation at a higher frequency is observable in the data from transducer J. Data from two supersonic speed conditions (13 300 and 14 800 rpm) are also presented in figure 12. In both of these conditions, the standard deviation does not show any sensitivity to angular location around the circumference, but the amplitude of the pressure and the general shape of the mean pressure distribution differ.

The spectral analysis and signal-enhancement analysis of transducer J at 11 850 rpm are presented in figure 13. The spectral analysis and harmonic analysis show that the first, second, and sixth harmonics are still significant components of the total pressure. The highest frequency signal is the 66th harmonic, and components at the 54th, 60th, and 72d harmonics are visible. There are 66 stators in the bypass duct and the 6 struts interact with these stators in such a manner that a band of pressure responses are presented around the 66th harmonic.

Fan-Blades/Potential-Field Interaction

One known source of far-field noise from a high-bypass engine is the interaction of the fan blades with the potential field caused by obstructions in the bypass duct, such as stators or support struts. This interaction has the capability of triggering acoustic spinning modes in the inlet duct. The noise from these duct modes propagates to the far field at the fan-blade passage frequency (BPF). Tyler and Sofrin (ref. 14) developed a criterion for determining if a particular duct mode could propagate out the front end of the inlet duct. This criterion for propagation is the cutoff ratio ξ given by

$$\xi = \frac{BM_T}{k'_{m,n}(1 - M_x^2)^{1/2}}$$

where M_T and M_x are the rotor-tip and duct-flow Mach numbers, respectively, and $k'_{m,n}$ is the mode eigenvalue for the cylindrical duct, determined from the interaction of the number of fan blades B and the flow field. When ξ equals or is greater than 1, the modal noise propagates. For example, a spinning mode resulting from the interaction between the 28 blades and the potential field from 6 struts would propagate down the duct at fan speeds greater than 10 750 rpm and at a mode number m of 22. Based on the results of the blade-mounted transducers, spinning modes resulting from blade interaction with 1, 2, 6, and 66 variations around the duct circumference (e.g., see fig. 9) would be strong candidates for excitation. Shown in table II are the cutoff fan speeds for these strong candidates and some other modes associated with peaks in the order analysis for different fan speeds. Included in this list is the cutoff frequency above which the rotor alone could excite a spinning mode.

In reference 15, based on relative sound power level, the BPF tone, which was integrated over the forward hemisphere, indicated peak responses at frequencies associated with the cuton of spinning modes m of 22 and 28. At 8 150 rpm ($m = 16$) no significant levels were reported and insufficient data were presented from 12 400 to 12 800 rpm to determine if a mode associated with $m = 26, -26$, or 27 caused a significant noise level in the far field.

To aid in determining the potential of exciting the spinning modes with $m = 27$, 26, and 22, the amplitude of the pressures for the 1st, 2d, and 6th harmonics (those harmonics h associated with the three modes) are plotted as a function of fan speed (adjusted for temperature corrections) in figures 14, 15, and 16, respectively. Shown in each of these figures is the fan speed at which the relative speed of the blade at the transducer location is equal to the speed of sound (Mach 1) and the cutoff speed of the spinning mode.

In figure 14 the amplitude at the fundamental fan frequency for transducers I and H shows a smooth increase until the relative speed of the blade reaches about Mach 1. Above the speed of sound the amplitude of the pressure varies with fan speed in a random manner. The pressure at transducer G starts to vary slightly before the local speed becomes Mach 1, and the pressure at transducer J does not show a variation and does not continue to increase in amplitude with fan speed. The change in amplitude of these pressures from the potential field would indicate that a new mechanism, such as local shocks in the transonic speed range, has complicated the pressure field on the blades. Discontinuities on the blades, such as the stiffeners and the pressure transducers, could be sources for triggering these local shocks. As can be seen in figure 14, these pressure variations start below the fan cutoff speed of 12 800 rpm for the $m = 27$ mode. In addition, over 12 percent of the outer span of the blade is traveling supersonically below the cutoff speed. The probability of this source being significant is low when considering that the local shocks vary the pressure levels on the blade and then the disturbance has to pass through a

shock wave before exciting the duct mode.

The characteristics for the second harmonic are similar to those discussed for the first harmonic. The pressures on the blade surface increase orderly with increasing fan speed. At about the point at which the local speed reaches Mach 1, the pressures no longer follow the orderly pattern. Transducer J does not show quite the amount of change as the other transducers, but at 13 300 rpm there is a large scatter in the data. As before, the cutoff speed for the $m = 26$ mode is above the speed at which the outer 12 percent of the blade is supersonic, suggesting that this is not a strongly excited mode in the duct.

The sixth harmonic also exhibits characteristics similar to those of the first and second harmonics (fig. 16). However, in this case the cutoff frequency for the $m = 22$ mode is well below the transonic speed range and is not affected by any shocks. Based on the pressures on the blades, it would appear that not only should the Tyler-Sofrin cutoff ratio be considered in determining if a spinning mode may be excited but also whether the local shock waves affect the source strength and whether the excitation mechanism has to pass through a shock front to develop.

Identification of the source of the fundamental fan frequency signal (one per revolution) has not been accomplished; however, based on the characteristics of the blade pressure, the source appears to be a flow-field type of disturbance similar to that of the six struts. The pressure remains as a peak in the spectrum throughout the entire fan speed range, although it does vary in amplitude in the transonic-supersonic range. The six struts cause an equal pressure disturbance at the outer edge of the blade, whereas the one-per-revolution pattern decreases from the outer edge toward the centerline. Also, the six-cycle amplitude varied considerably at the trailing edge in the transonic-supersonic range, whereas the one-cycle amplitude did not vary much at all. All these effects suggest a flow-field distortion caused by a mechanism originating at the periphery of the blade, such as might be caused by the duct being slightly eccentric.

Comparison of Flight and Tunnel Tests in the Transonic Range

The inlet was designed to operate over the entire range of test environments—static, wind tunnel, and flight with a minimum of effect at the fan face. As shown in figure 8 of reference 15, the Mach number and pressure ratio at the fan face would be the same for the same mass flow in the engine. Also, the boundary layer at the fan location would change only from about 0.99 cm (0.39 in.) in flight to 1.17 cm (0.46 in.) statically. Experimental data, also from reference 15, showed that the fan operating line was about the same for flight and ground testing. One difference noted that might affect the blade pressure measurements was the tip relative incidence angle of the mean flow to the blades. Because of a difference in the stagnation pressure between ground and flight tests, this angle varied by about 1½° at 12 000 rpm. This difference in incidence angle is expected to affect the broadband noise levels in the far field caused by inflow effects.

Some results from the tunnel tests have been presented in references 7 and 9. In the study of reference 7, it was determined that once a minimum forward speed was reached (in this engine-inlet combination it was about 10 m/sec) the blade fluctuating pressures were unaffected by changes in the tunnel speed. Therefore, the differences between the tunnel speed of 44 m/sec and the flight speed of 67 m/sec are not considered to have a significant effect on the blade pressure data. Comparisons for the subsonic range showed good agreement between the spectra, mean and standard deviations, and the harmonic-order analysis from the tunnel tests and flight results (ref. 9). This would indicate that although there is a slight variation in the inlet flow between flight and ground, the blade-mounted transducers were not very sensitive to this difference at subsonic speeds.

Figure 17 shows the results from transducer H (leading edge of blade) in the transonic fan tip-speed range in the wind tunnel. The spectra (fig. 17(a)) do not indicate an observable peak at the sixth harmonic that is observable in flight. The peak at the fundamental frequency remains. Figure 17(b) shows the mean and standard deviations in which the large one-cycle observation may be observed in the mean deviation and the standard deviation varies with circumferential location. The order analysis points out that the response at the fundamental fan frequency is primarily periodic. There is no other periodic response within 10 dB of this value. The one-per-revolution oscillation has about the same magnitude in the tunnel and flight tests.

At transducer J (located near the trailing edge of the blade, as shown in fig. 18), large peaks in the pressure response show up at frequencies of 1, 6, and 66 cycles per revolution; and the shape of the mean- and standard-deviation plots are similar to those in flight (fig. 12). In addition to these three peaks, peak responses at ±6 harmonic orders relative to the 66th harmonic show up as high peaks in the order analysis. At this fan speed only the sixth order would be exciting a spinning mode; however, it would not be expected to be strongly excited since the excitation is not even seen at the leading edge of the fan blade. Also, as was pointed out earlier in the transonic range, the magnitude of this sixth harmonic begins to vary greatly with frequency on the blade surface in the transonic-supersonic range. Because of these variations, the use of the blade-mounted transducers in the transonic range

is greatly reduced as a measurement of sources for the spinning modes.

Concluding Remarks

A study has been conducted to evaluate the characteristics of pressure measurements on the surface of the fan blades of a turbofan engine as a potential source of acoustic noise. Data have been obtained from the fan of a JT15D engine flown on the wing of an OV-1B airplane. Fan-blade tip speeds varied from the subsonic to the supersonic speed ranges. Analysis of the data from miniature pressure transducers mounted directly on the fan blades was made by using spectral analysis and enhanced-signal data-reduction methods. Some comparisons with wind-tunnel data were made.

In the subsonic blade tip speed ranges, the pressures on the surface increase orderly with increasing fan speed for the peak amplitude frequencies. For the JT15D engine, these frequencies occur at the fan rotational speed (at the 2d, 6th, and 66th harmonics). As the fan speeds increase into the transonic and supersonic tip speed ranges, the pressures on the blade surfaces no longer follow an orderly pattern with increasing fan speed. In the transonic range there is a large increase in the broadband fluctuating surface pressures over those seen in either the subsonic or supersonic ranges. At transonic tip speeds, according to the Tyler-Sofrin criterion, only the sixth harmonic should cause fan noise to propagate out the duct. The amplitudes differed between the wind tunnel and flight data at the leading edge of the blade but agreed at the trailing edge. Far-field data from the wind tunnel and flight did compare well at these speeds, implying that another mechanism not directly related to blade pressure may be the primary source of fan noise in this range.

The one-per-revolution oscillation is very similar to the six-per-revolution oscillation (attributed to the six internal support struts) and varies only in that the one-per-revolution signal amplitude is at a maximum at the tip and decreases in amplitude down the span. The six-per-revolution amplitude is relatively constant over the span. This similarity suggests a flow-field distortion, similar to the six-per-revolution signal, that is generated only at the periphery of the fan blades, such as might be caused by an eccentric duct.

Langley Research Center
National Aeronautics and Space Administration
Hampton, VA 23665
November 20, 1984

References

1. Feiler, Charles E.; and Groeneweg, John F.: *Summary of Forward Velocity Effects on Fan Noise.* NASA TM-73722, 1977.
2. Povinelli, Frederick P.; and Dittmar, James H.: *Installation Caused Flow Distortion and Its Effect on Noise From a Fan Designed for Turbofan Engines.* NASA TM X-68105, 1972.
3. Hanson, Donald B.: *The Spectrum of Turbomachine Rotor Noise Caused by Inlet Guide Vane Wakes and Atmospheric Turbulence.* HSER 6191, Hamilton Standard Div., United Aircraft Corp., May 14, 1973.
4. Hanson, Donald B.: *Study of Noise Sources in a Subsonic Fan Using Measured Blade Pressures and Acoustic Theory.* NASA CR-2574, 1975.
5. Rogers, D. F.; and Ganz, U. W.: Aerodynamic Assessment of Methods To Simulate Flight Inflow Characteristics During Static Engine Testing. AIAA-80-1023, June 1980.
6. Preisser, J. S.; Schoenster, J. A.; Golub, R. A.; and Horne, C.: Unsteady Fan Blade Pressure and Acoustic Radiation From a JT15D-1 Turbofan Engine at Simulated Forward Speed. AIAA-81-0096, Jan. 1981.
7. Schoenster, James A.: *Fluctuating Pressures on Fan Blades of a Turbofan Engine—Static and Wind-Tunnel Investigations.* NASA TP-1976, 1982.
8. Chestnutt, David, ed.: *Flight Effects of Fan Noise.* NASA CP-2242, September 1982.
9. Schoenster, James A.: Fluctuating Pressure Measurements on the Fan Blades of a Turbofan Engine During Ground and Flight Tests. AIAA-83-0679, Apr. 1983.
10. Golub, Robert A.; and Preisser, John S.: *Test-Engine and Inlet Performance of an Aircraft Used for Investigating Flight Effects on Fan Noise.* NASA TP-2254, 1984.
11. Grumman Aerospace Corp.: *Final Report of the Feasibility Study for the Installation and Test of a Pratt and Whitney Turbofan Engine on a Mohawk Aircraft.* NASA CR-145314, 1978.
12. Englund, David R.; Grant, Howard P.; and Lanati, George A.: *Measuring Unsteady Pressure on Rotating Compressor Blades.* NASA TM-79159, 1979.
13. Knight, Vernie H., Jr.: In-Flight Jet Engine Noise Measurement System. *Instrumentation in the Aerospace Industry—Volume 27, Advances in Test Measurement—Volume 18, Part One, Proceedings of the 27th International Instrumentation Symposium*, Instrum. Soc. America, 1981, pp. 381–386.
14. Tyler, J. M.; and Sofrin, T. G.: Axial Flow Compressor Noise Studies. *SAE Trans.*, vol. 70, 1962, pp. 309–332.
15. Preisser, John S.; and Chestnutt, David: Flight Effects on Fan Noise With Static and Wind Tunnel Comparisons. AIAA-83-0678, Apr. 1983.

TABLE I. SPECIFICATIONS OF JT15D

Fan speed (max.), rpm	16 000
Fan pressure ratio	1.5
Bypass ratio (max.)	3.3
Number of fan blades	28
Fan diameter, cm	53.3
Hub-tip ratio	0.405
Number of bypass-stator vanes	66
Number of core-stator vanes	[a]71
Rotor/bypass-stator spacing	[b]1.83
Rotor/core-stator spacing	0.63
Compressor speed (max.), rpm	32 760
Core exhaust area, m^2	0.051
Bypass exhaust area, m^2	0.092
Thrust capability, N	9790

[a]Production engine has 33 core-stator vanes.
[b]Production-engine core-stator spacing is 0.28, normalized to fan-blade root chord.

TABLE II. POTENTIAL ACOUSTIC PROPAGATING SPINNING MODES

[28 fan blades]

Harmonic order of fan speed, h	Mode number, m	Fan cutoff speed, rpm
	28	13 200
1	27	12 800
2	26	12 400
[a]6	22	10 750
12	16	8 150
54	−26	12 400
60	−32	14 750
[b]66	−38	(c)
72	−44	(c)

[a]Number of support struts in bypass duct.
[b]Number of stators in bypass duct.
[c]Out of operating range.

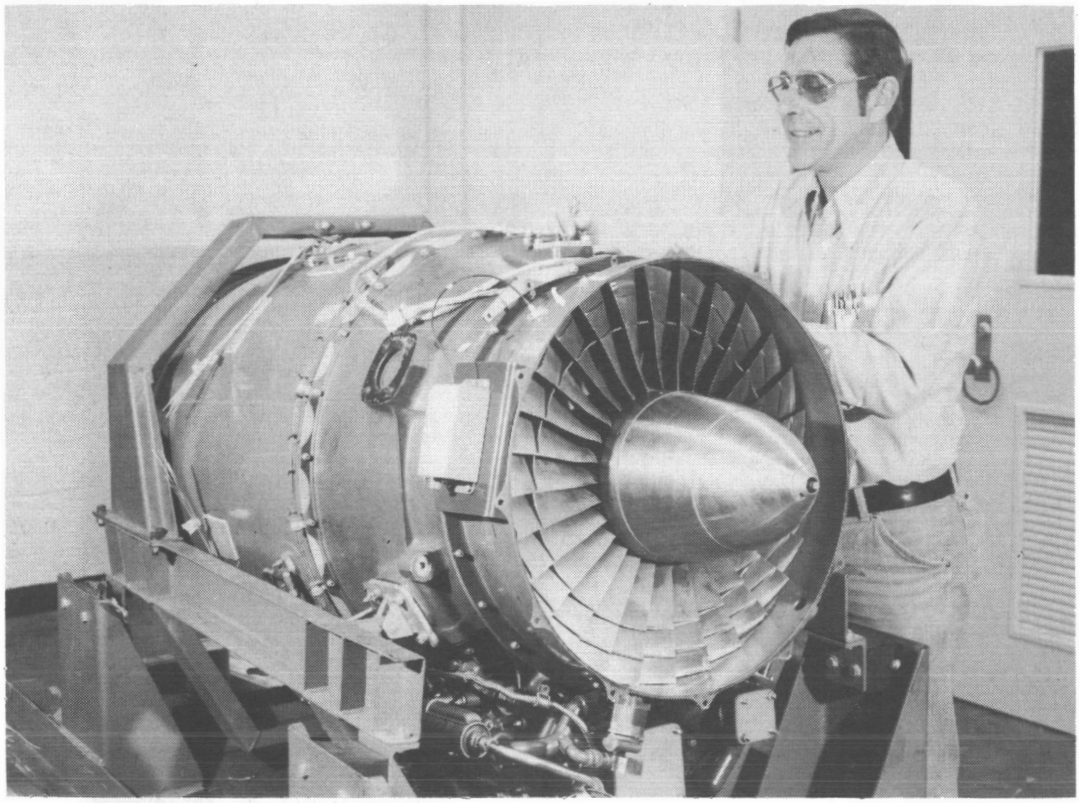

L-80-950

Figure 1. JT15D engine with nacelle and inlet duct removed.

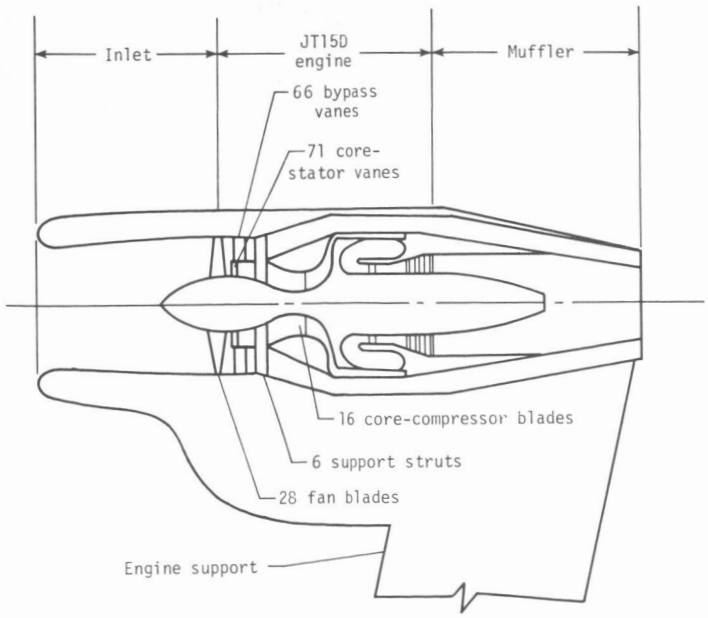

Figure 2. Schematic cross-sectional view of JT15D engine in tunnel configuration.

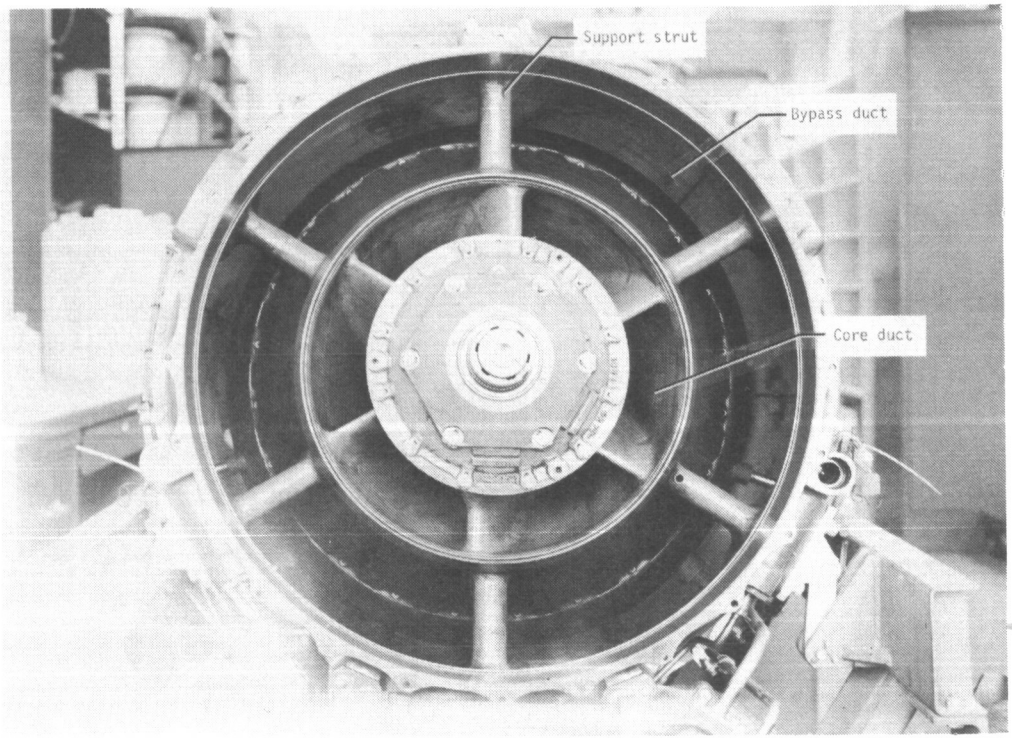

L-80-4221

Figure 3. Internal structure of JT15D engine showing six support struts in bypass duct.

L-80-3565

Figure 4. JT15D engine mounted on wing pylon of OV-1B airplane.

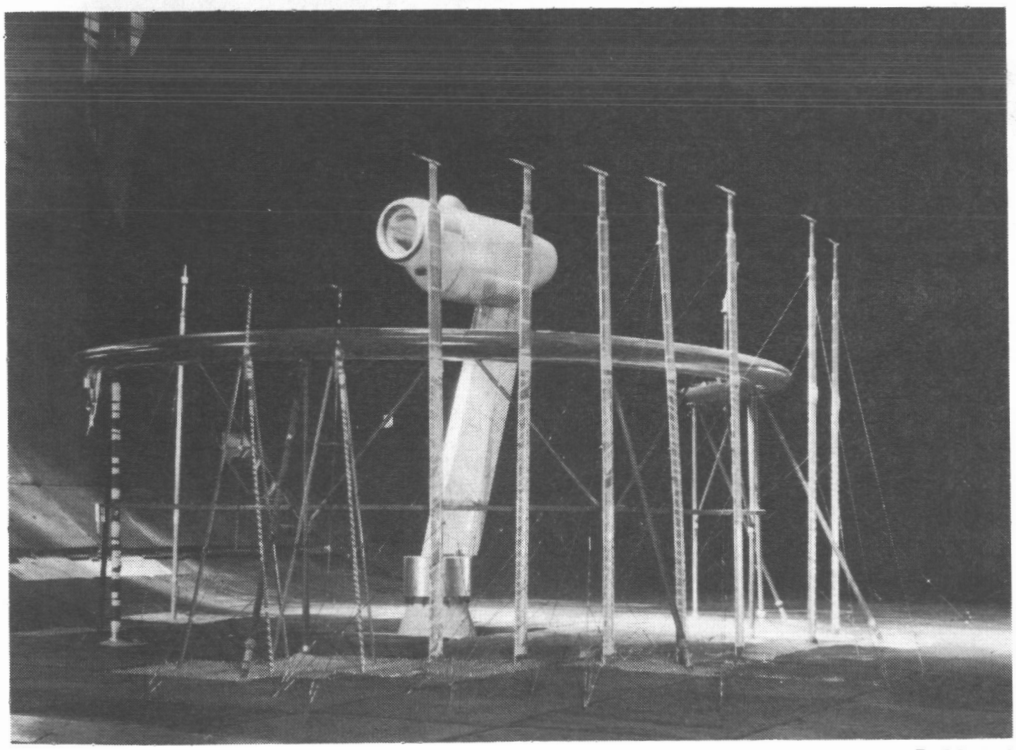

L-82-118

Figure 5. JT15D engine mounted in the Ames 40- by 80-Foot Wind Tunnel.

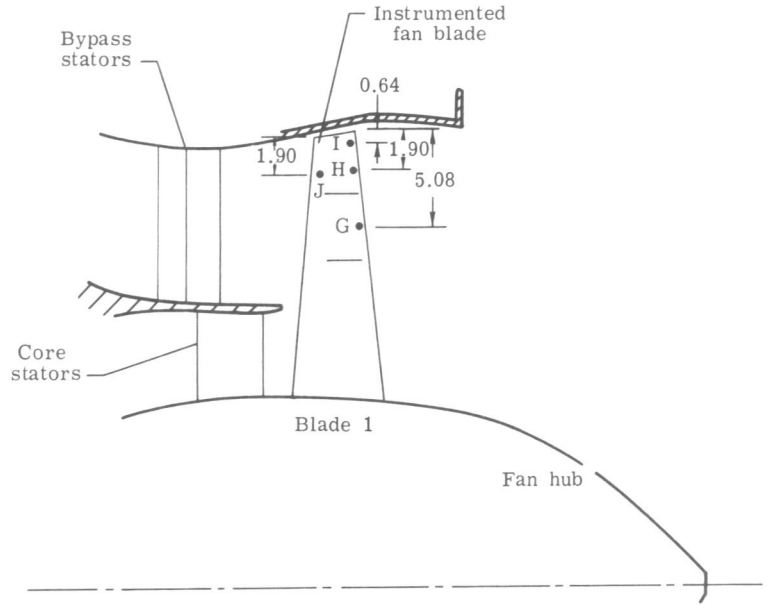

Figure 6. Schematic drawing showing locations of fan-blade-mounted transducers. All blade transducers are 0.38 cm from leading edge or 0.89 cm from trailing edge. Dimensions are given in centimeters.

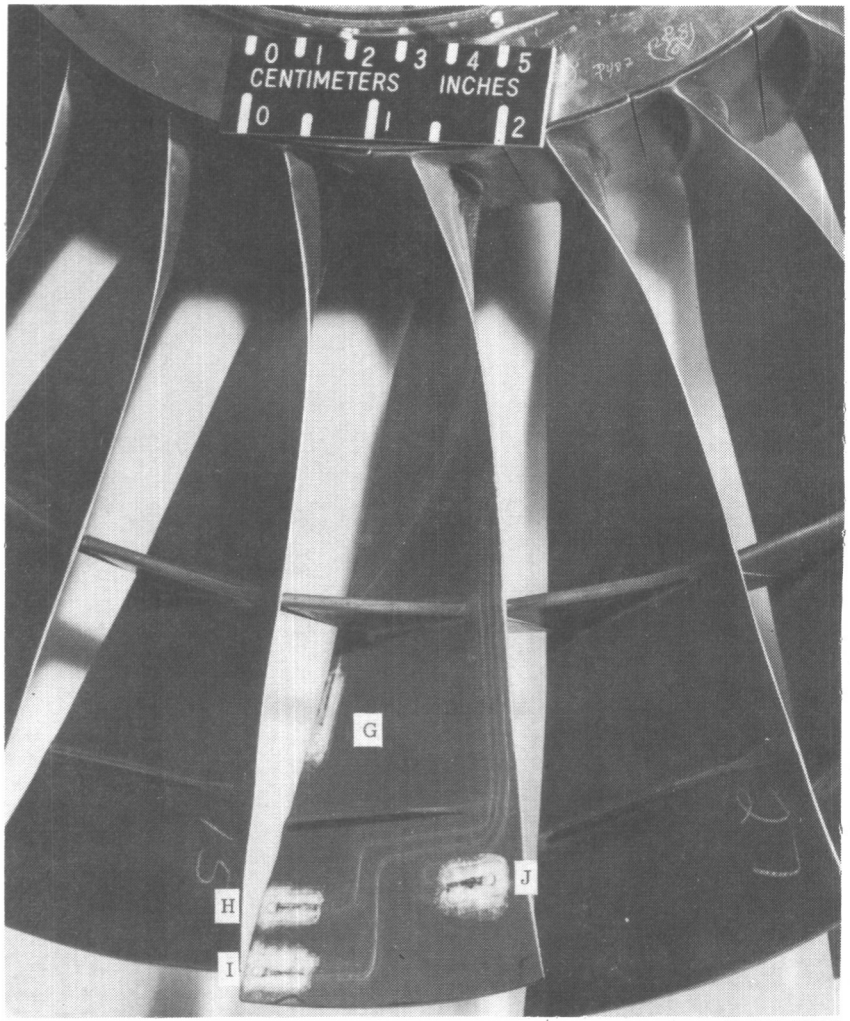

L-80-4548

Figure 7. Fan-blade-mounted transducers used in this study.

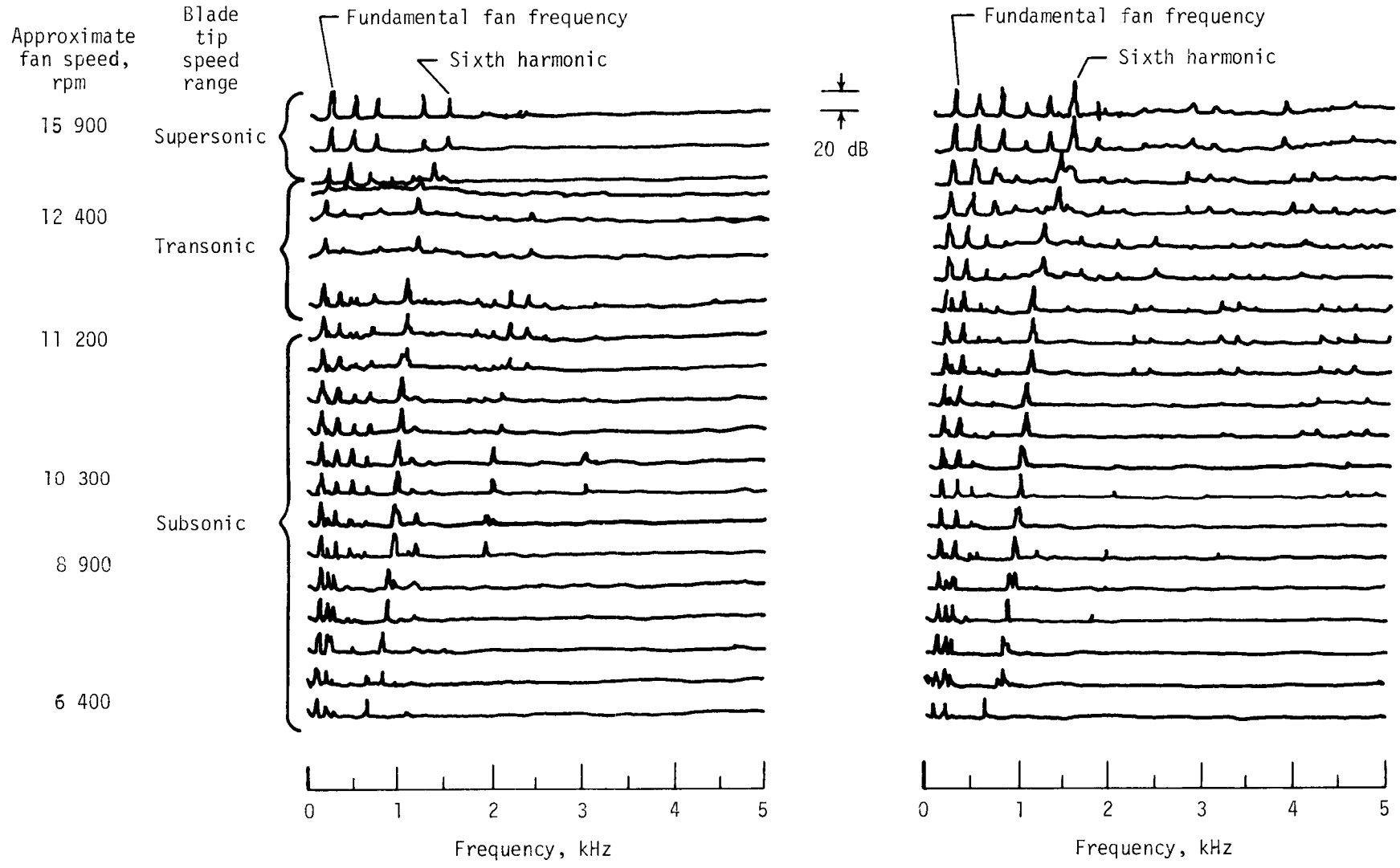

(a) Transducer H (leading edge).

(b) Transducer J (trailing edge).

Figure 8. Spectral time history of fan-blade-mounted transducers from fan-speed sweep during flight. Altitude, 100 m; forward speed, 67 m/sec (130 knots).

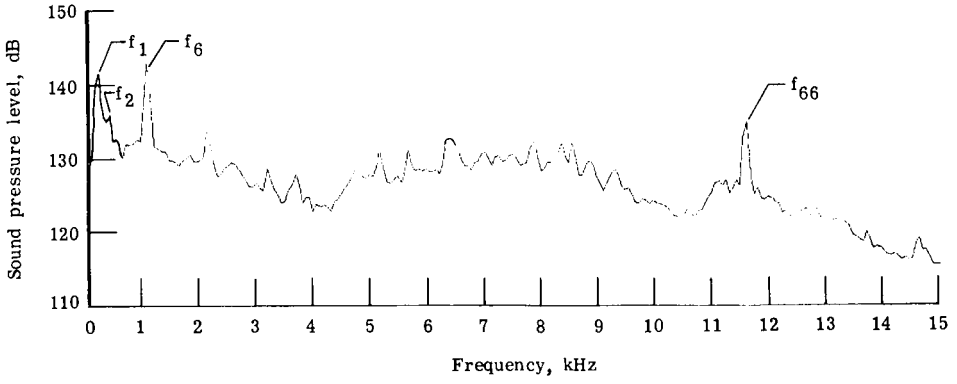

(a) Spectral analysis of overall signal.

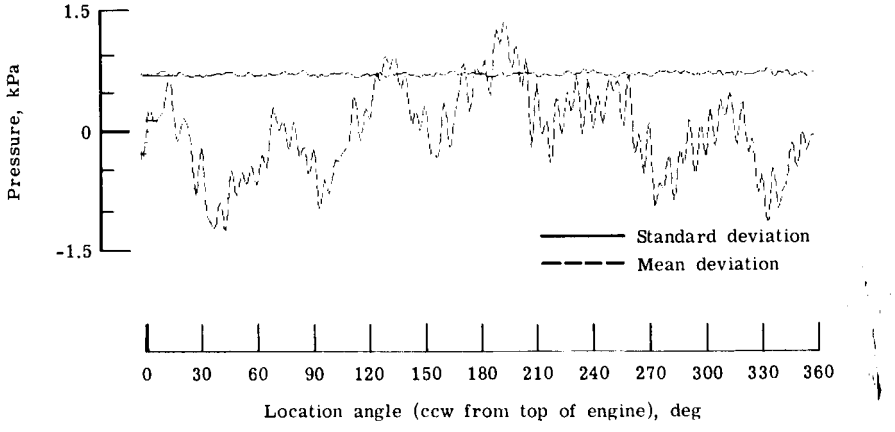

(b) Standard and mean deviations of enhanced signal.

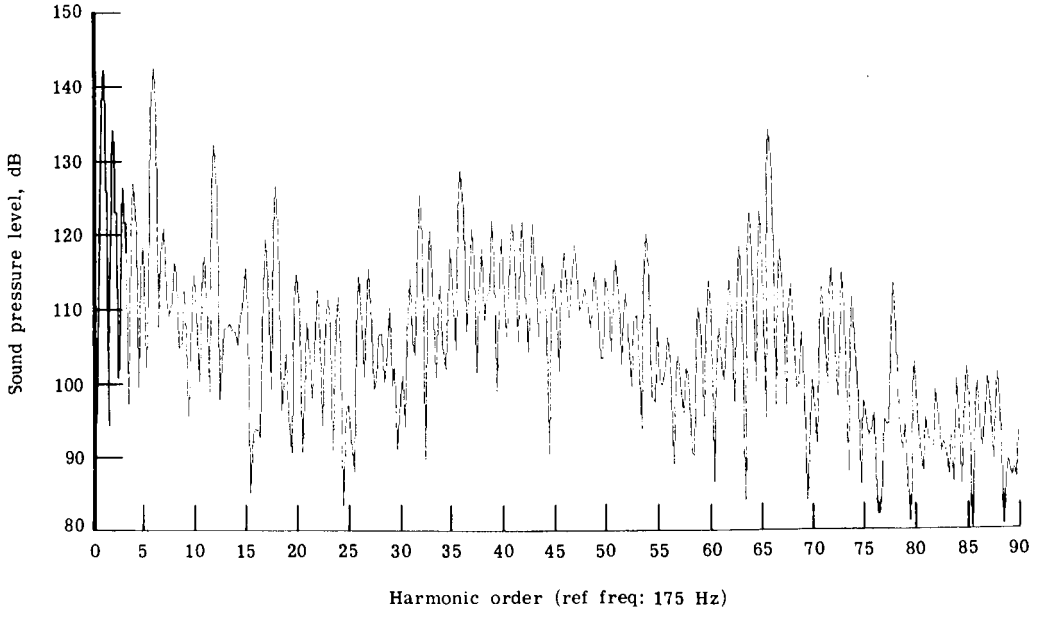

(c) Harmonic-order analysis of enhanced signal.

Figure 9. Data analysis for transducer H in flight at fan speed of 10 400 rpm.

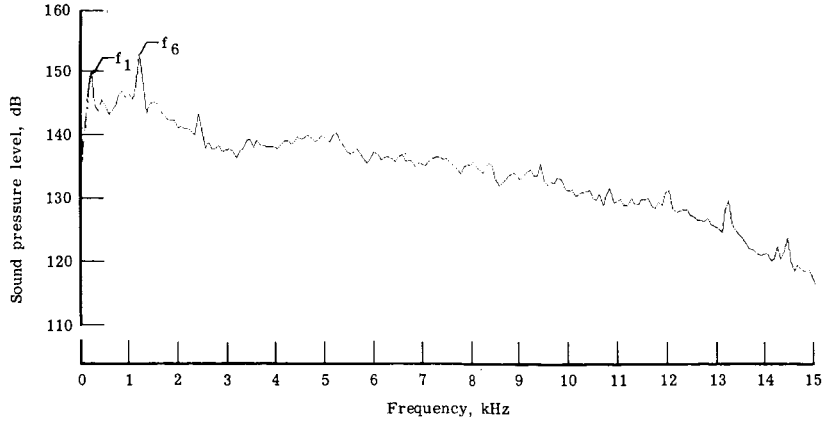

(a) Spectral analysis of overall signal.

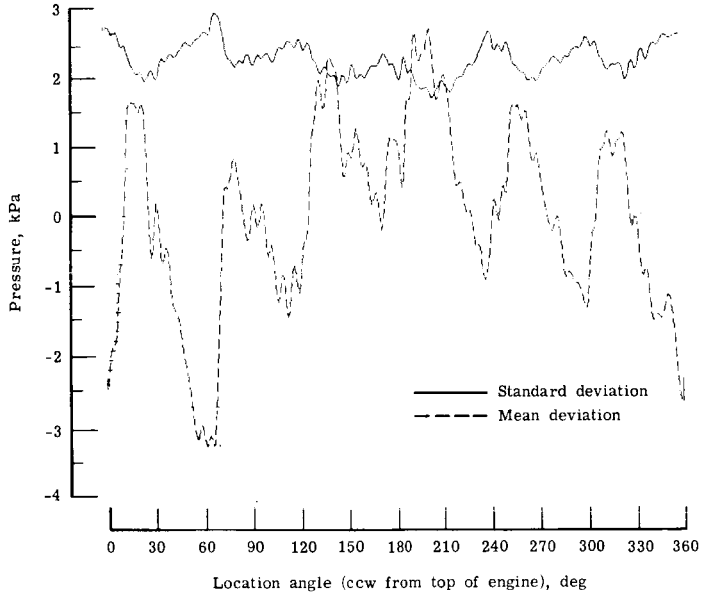

(b) Standard and mean deviations of enhanced signal.

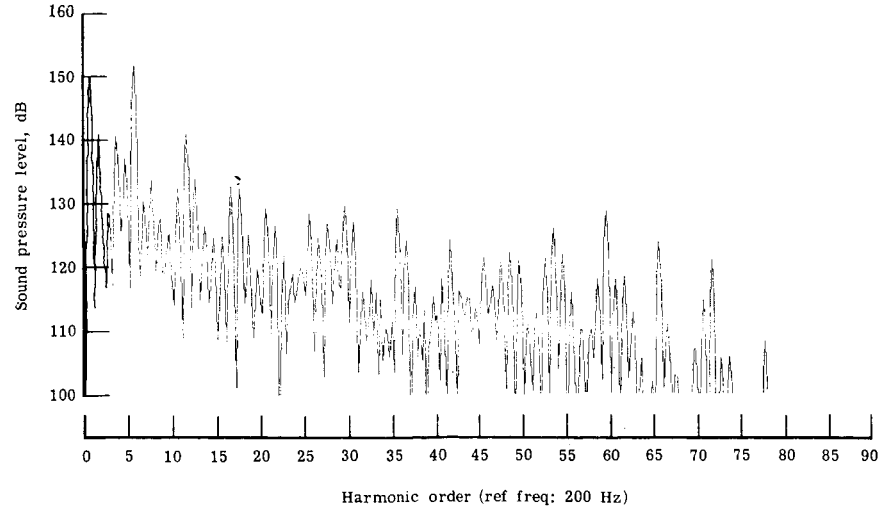

(c) Harmonic-order analysis of enhanced signal.

Figure 10. Data analysis for transducer H in flight at fan speed of 11 850 rpm.

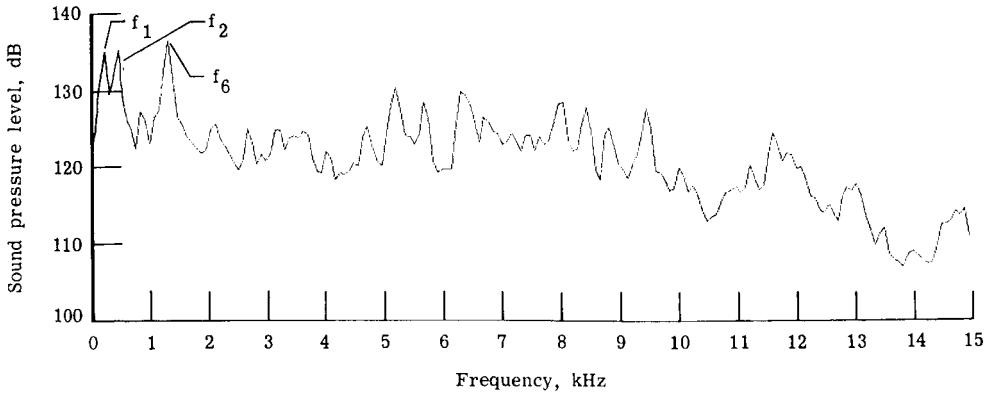

(a) Spectral analysis of overall signal.

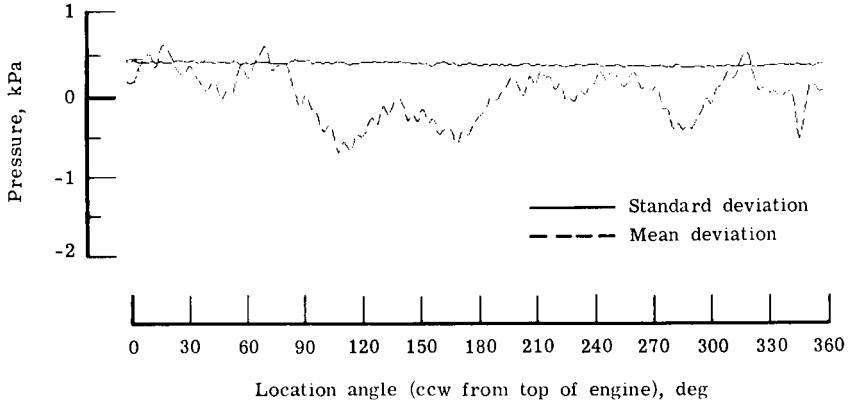

(b) Standard and mean deviations of enhanced signal.

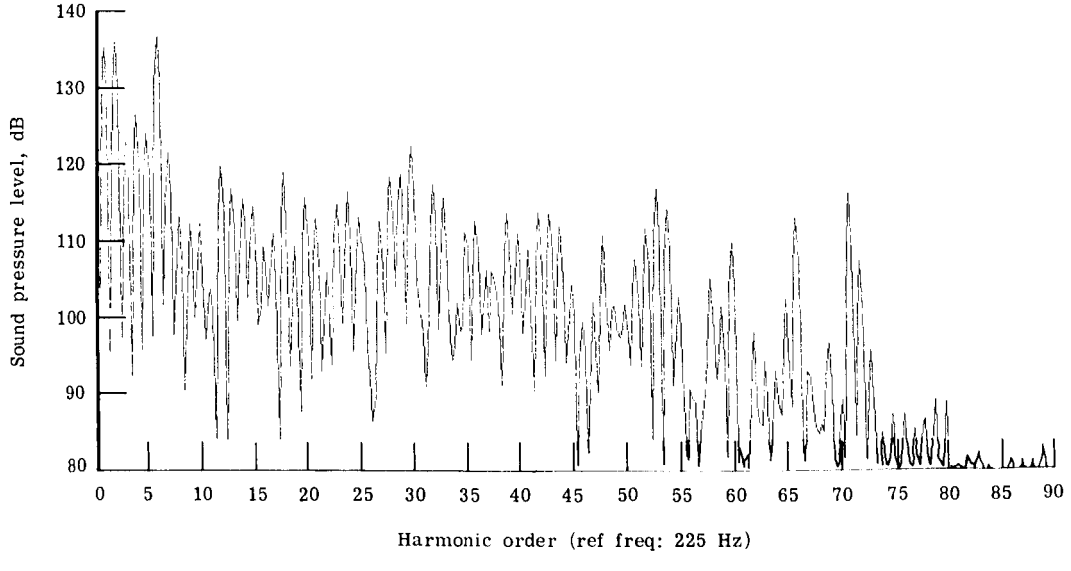

(c) Harmonic-order analysis of enhanced signal.

Figure 11. Data analysis for transducer H in flight at fan speed of 13 300 rpm.

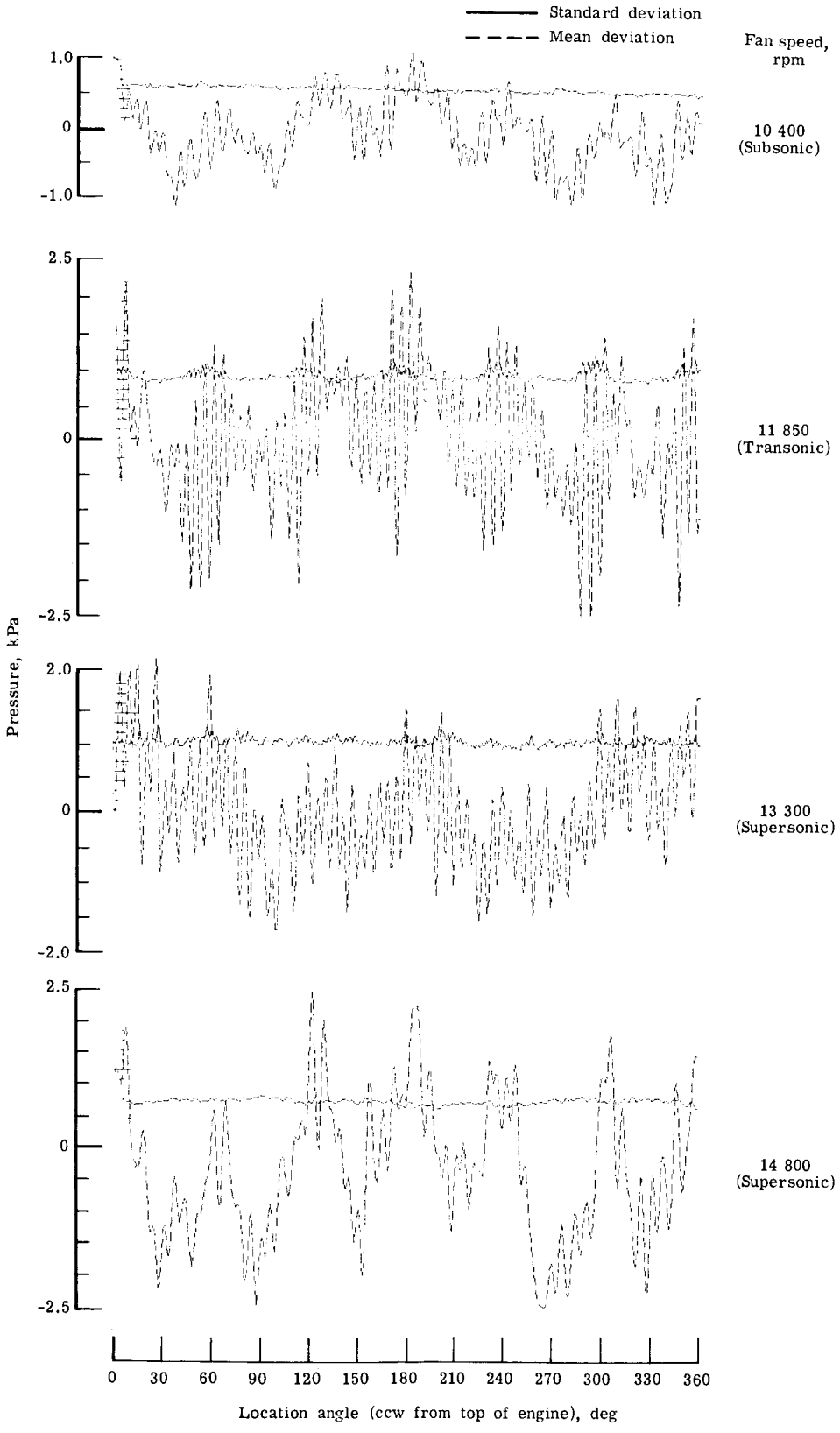

Figure 12. Mean and standard deviations of transducer J for subsonic, transonic, and supersonic fan speeds.

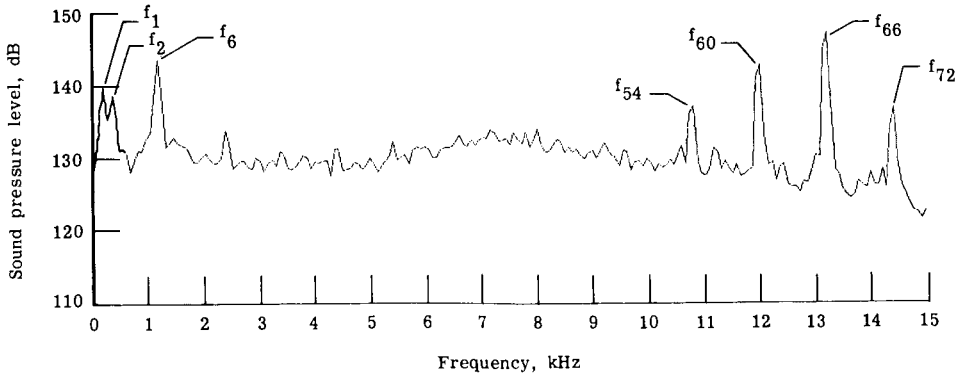

(a) Spectral analysis of overall signal.

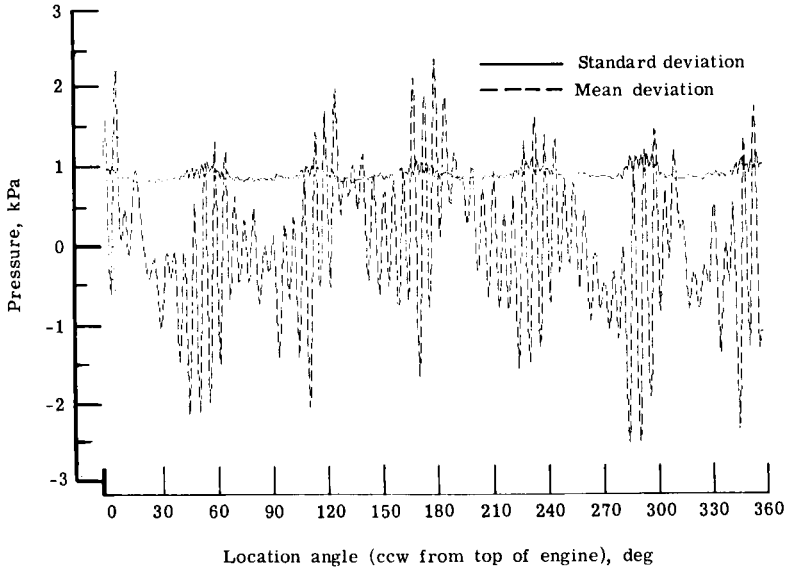

(b) Standard and mean deviations of enhanced signal.

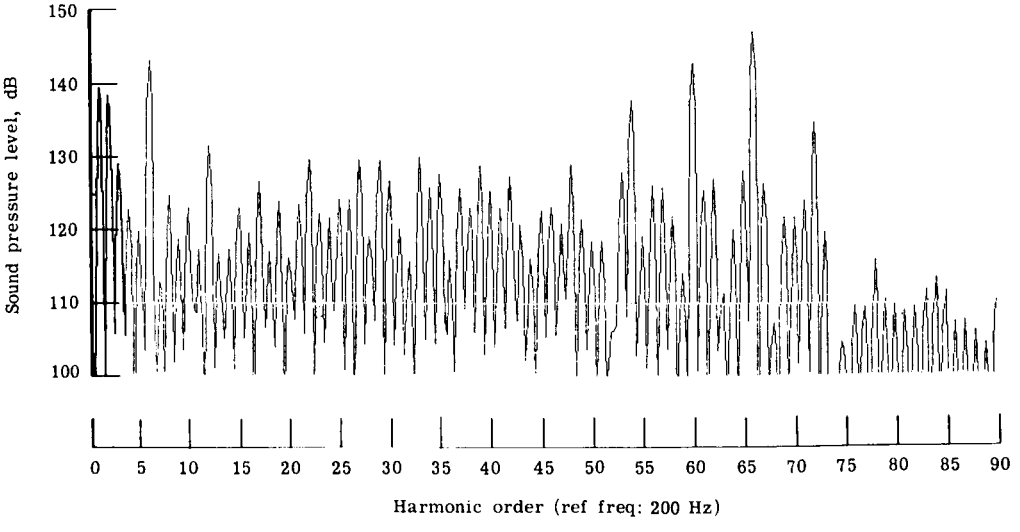

(c) Harmonic-order analysis of enhanced signal.

Figure 13. Data analysis for transducer J in flight at fan speed of 11 850 rpm.

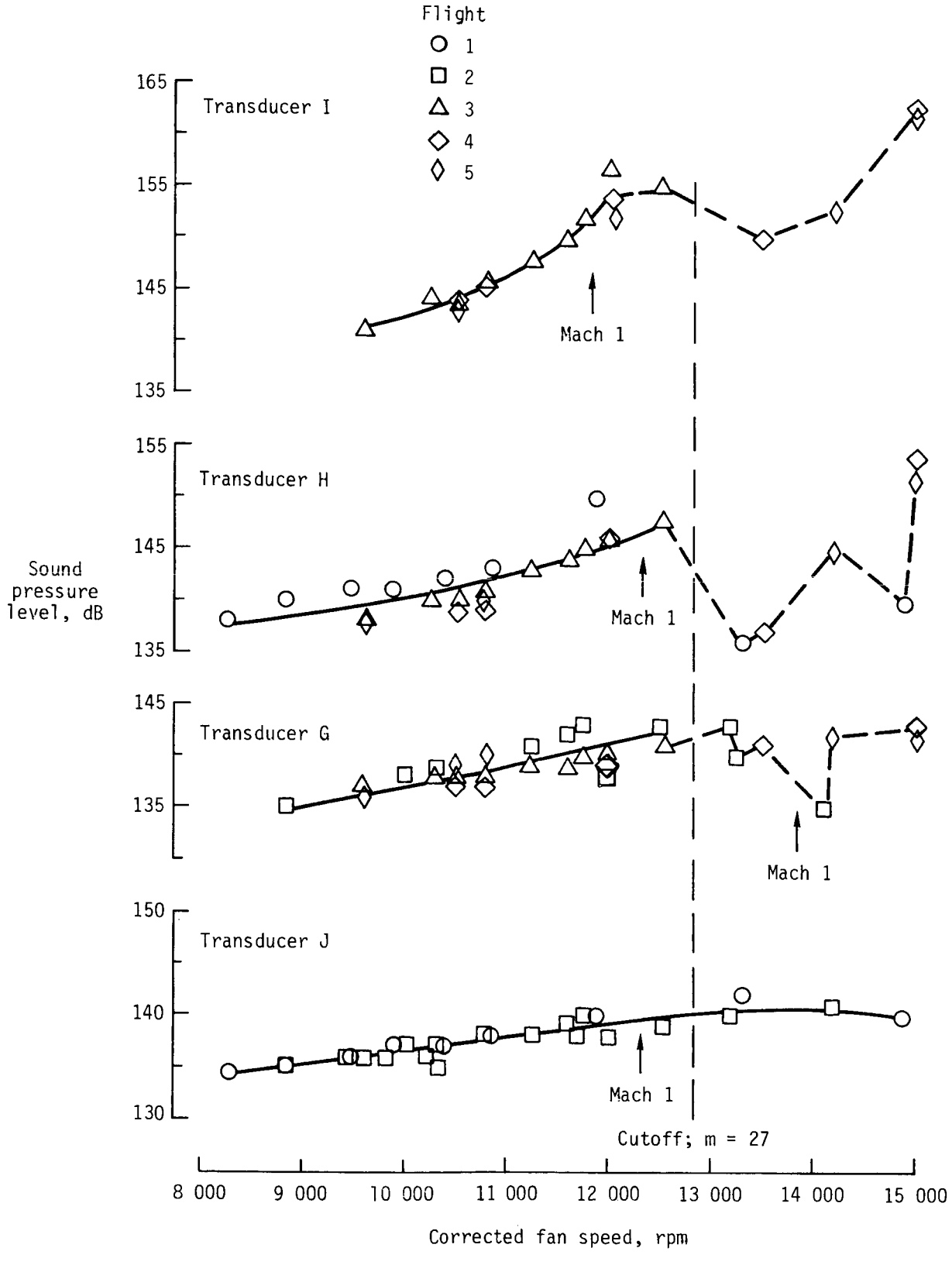

Figure 14. Amplitude of fluctuating pressure at fundamental fan frequency on fan blade of JT15D engine during flight.

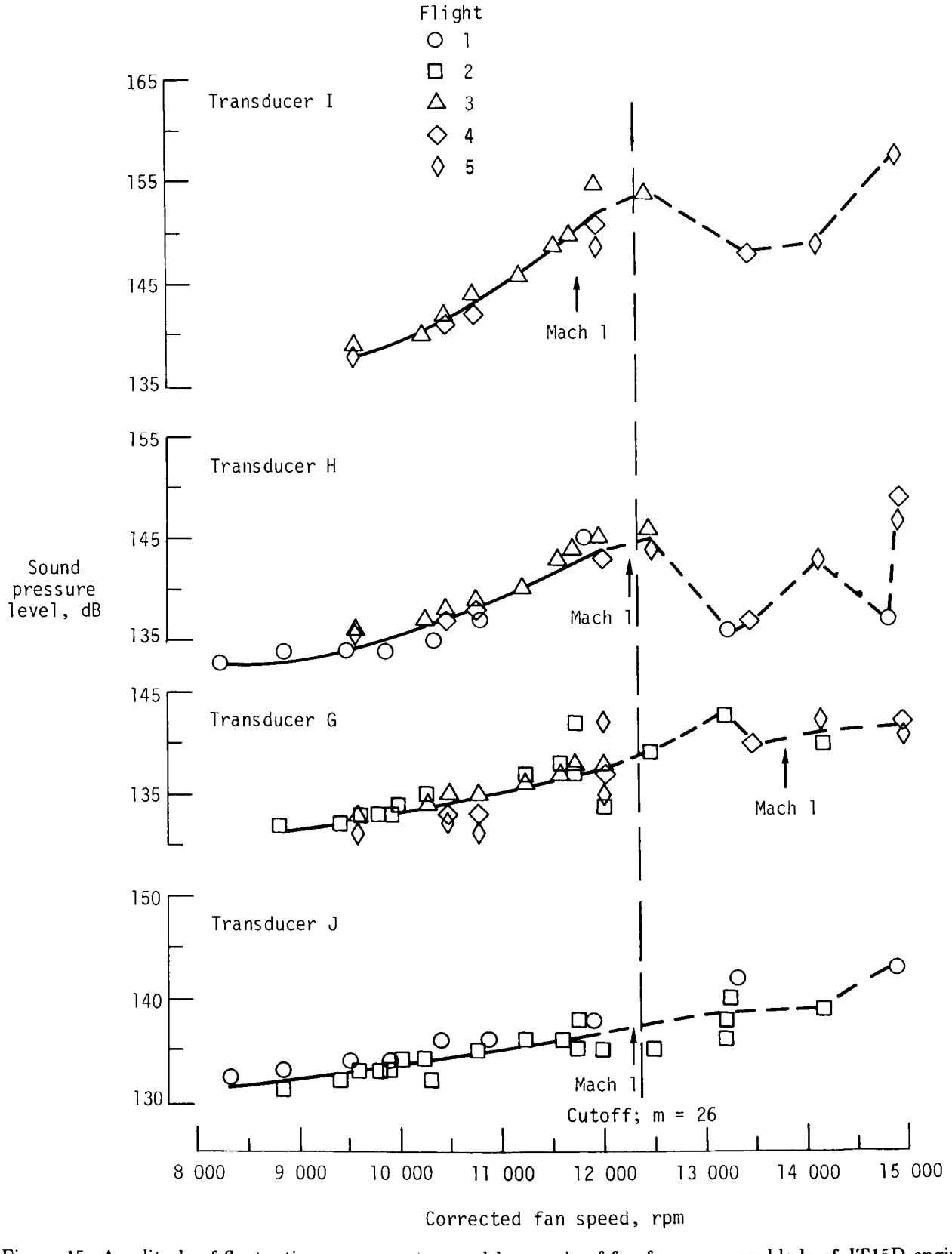

Figure 15. Amplitude of fluctuating pressure at second harmonic of fan frequency on blade of JT15D engine during flight.

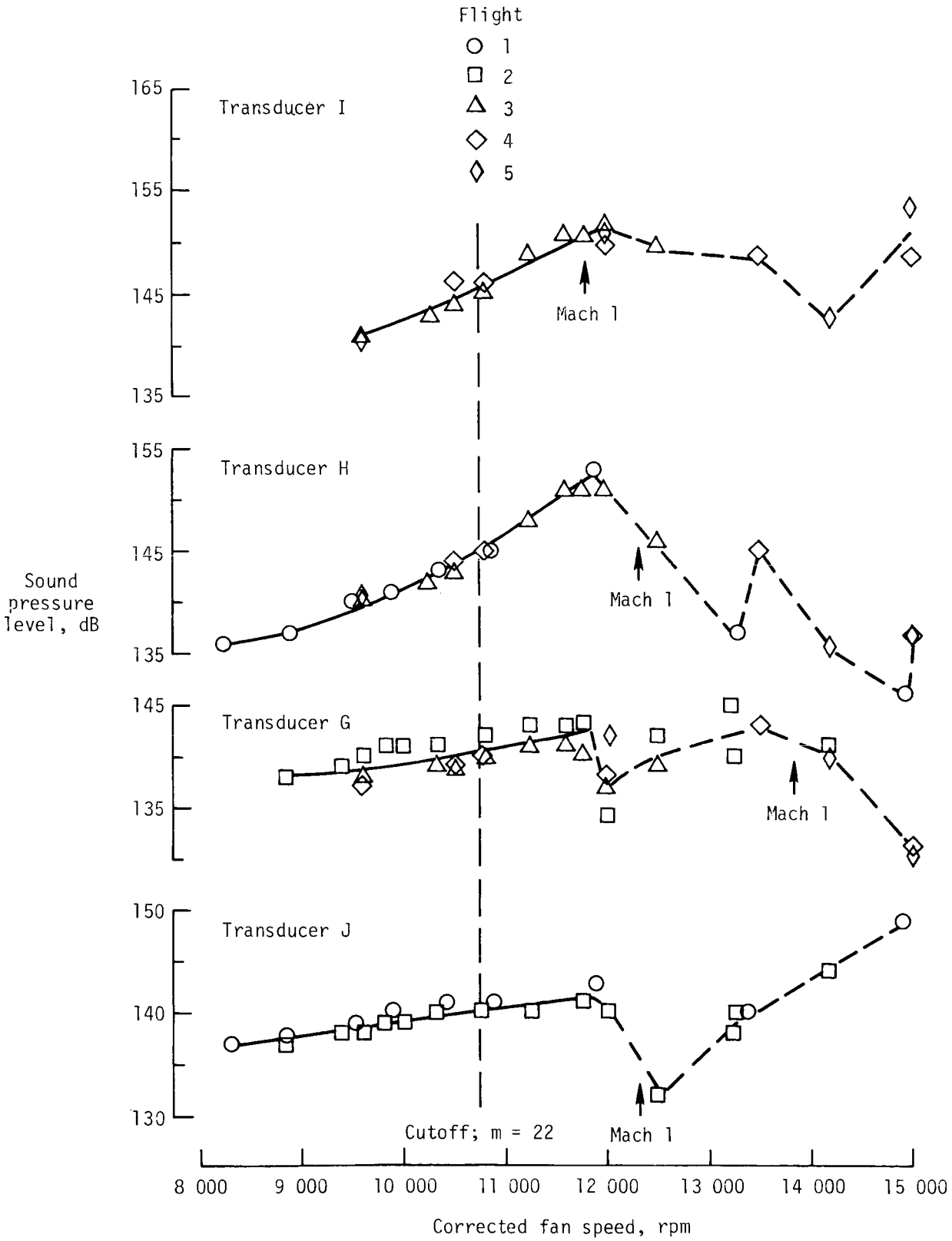

Figure 16. Amplitude of fluctuating pressure at sixth harmonic of fan frequency on blade of JT15D engine during flight.

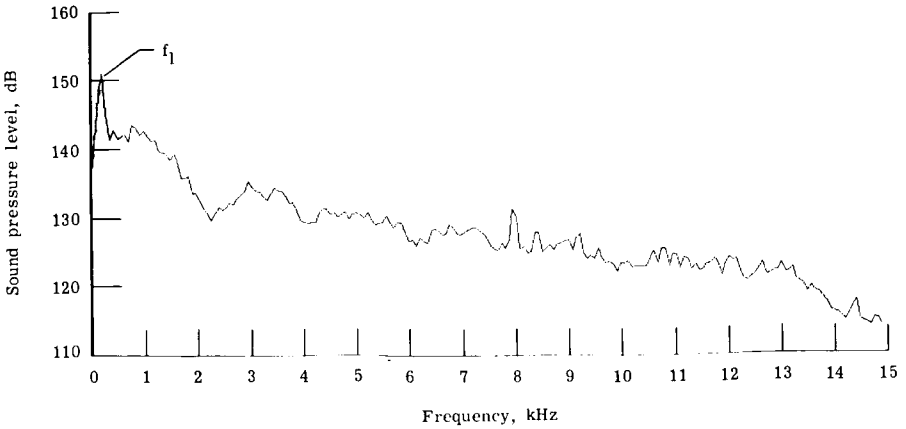

(a) Spectral analysis of overall signal.

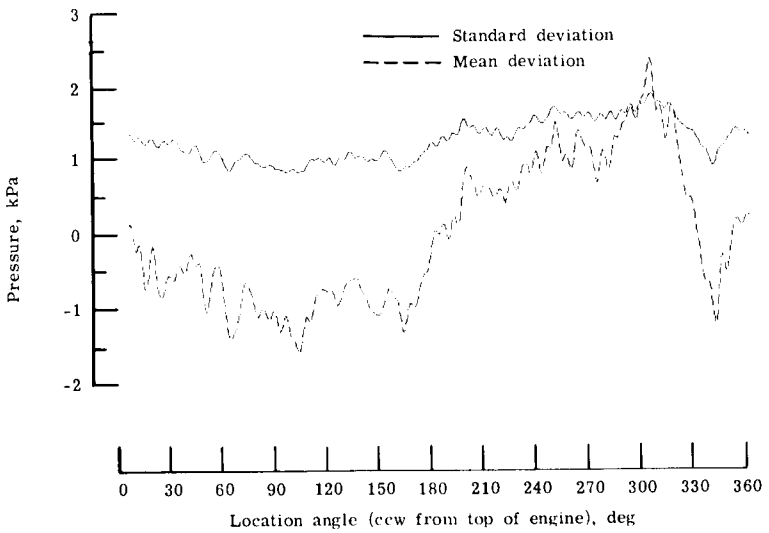

(b) Standard and mean deviations of enhanced signal.

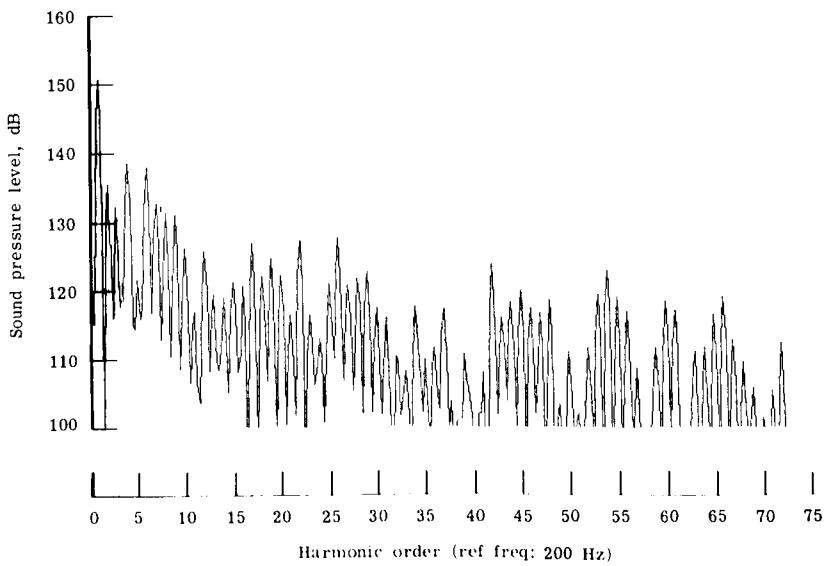

(c) Harmonic-order analysis of enhanced signal.

Figure 17. Data analysis for transducer H in wind tunnel at fan speed of 11 975 rpm. Tunnel speed, 44 m/sec.

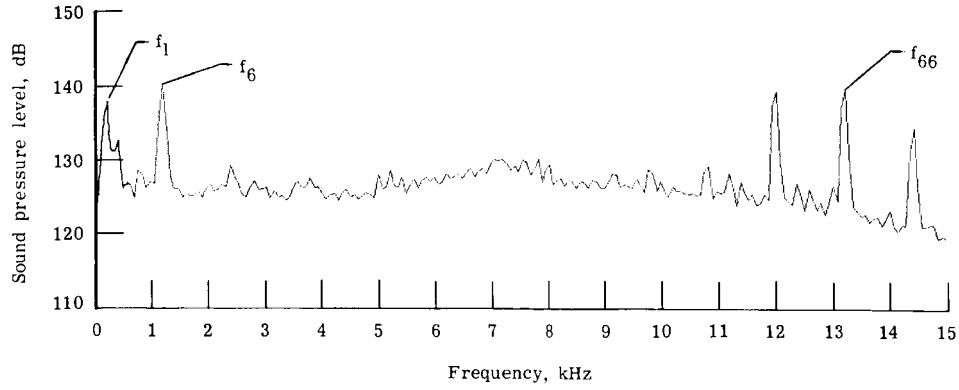

(a) Spectral analysis of overall signal.

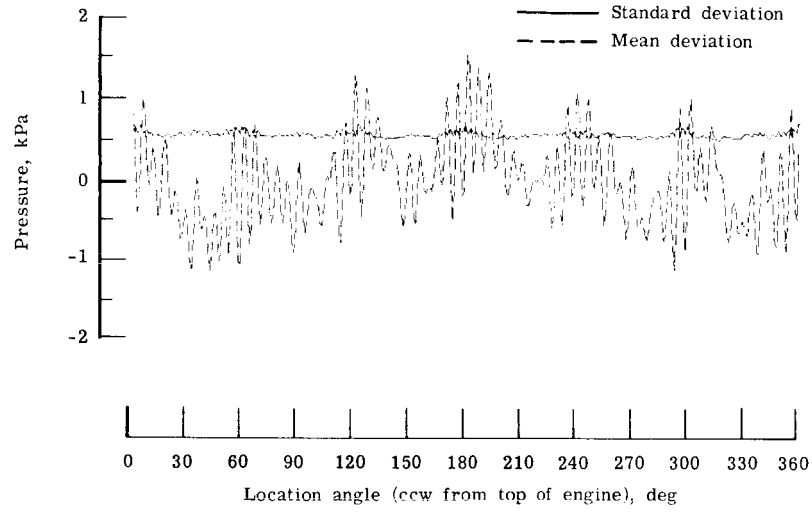

(b) Standard and mean deviations of enhanced signal.

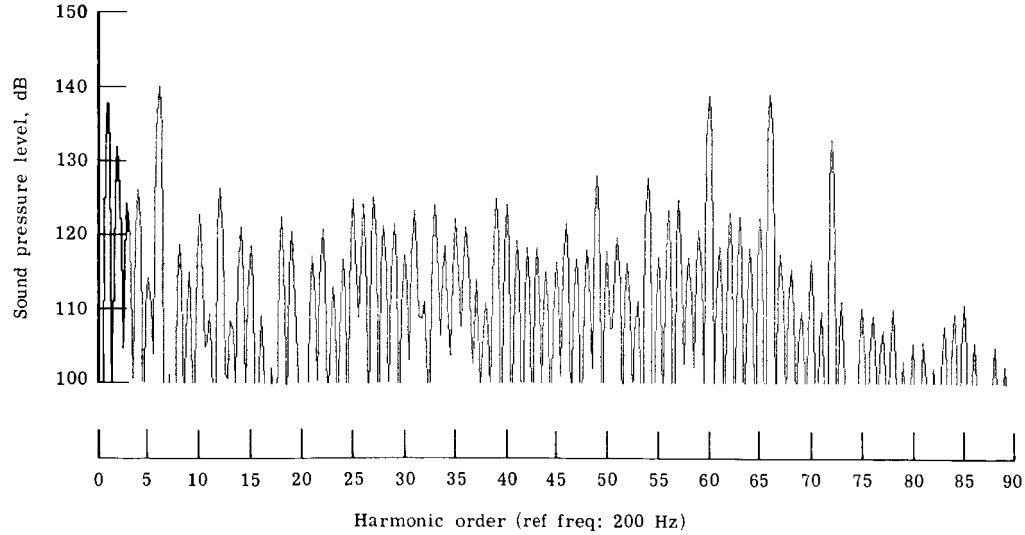

(c) Harmonic-order analysis of enhanced signal.

Figure 18. Data analysis for transducer J in wind tunnel at fan speed of 11 975 rpm. Tunnel speed, 44 m/sec.

1. Report No.	2. Government Accession No.	3. Recipient's Catalog No.
NASA TP-2381		

4. Title and Subtitle	5. Report Date
Fluctuating Pressures on Fan Blades of a Turbofan Engine—Flight Test Investigation	February 1985
	6. Performing Organization Code: 505-31-33-13
7. Author(s): James A. Schoenster	8. Performing Organization Report No.: L-15700
9. Performing Organization Name and Address: NASA Langley Research Center, Hampton, VA 23665	10. Work Unit No.
	11. Contract or Grant No.
12. Sponsoring Agency Name and Address: National Aeronautics and Space Administration, Washington, DC 20546	13. Type of Report and Period Covered: Technical Paper
	14. Sponsoring Agency Code

15. Supplementary Notes

16. Abstract

Miniature pressure transducers were used to measure the fluctuating pressure on the fan blades of a JT15D engine in flight to aid in understanding fan-noise generation. Although the blade pressures can be considered very useful in determining far-field noise sources in the subsonic fan-blade tip speeds, other mechanisms, such as shock waves in the transonic and supersonic fan-blade tip speeds, limit their usefulness in these higher speed ranges.

17. Key Words (Suggested by Authors(s))
Turbofan noise sources
Fan-blade-mounted pressure transducers
Static and flight fan noise testing
Turbofan inlet turbulence

18. Distribution Statement
Unclassified—Unlimited

Subject Category 71

19. Security Classif.(of this report)	20. Security Classif.(of this page)	21. No. of Pages	22. Price
Unclassified	Unclassified	24	A02

For sale by the National Technical Information Service, Springfield, Virginia 22161

NASA-Langley, 1985

NASA